

AR-010-605

**O
T
S
D**

Numerical Simulation of Detonation in
Condensed Phase Explosives

D.A. Jones, G. Kemister and
R.A.J. Borg

DSTO-TR-0705

APPROVED FOR PUBLIC RELEASE

© Commonwealth of Australia

Numerical Simulation of Detonation in Condensed Phase Explosives

D.A. Jones, G. Kemister and R.A.J. Borg

**Weapons Systems Division
Aeronautical and Maritime Research Laboratory**

DSTO-TR-0705

ABSTRACT

This report describes the development of a two-dimensional multi-material Eulerian hydrocode to model the effects of detonating condensed phase explosives on surrounding materials. The code solves the Euler equations for the conservation of mass, momentum, and energy for an inviscid, compressible fluid. Operator splitting is used to reduce the two-dimensional calculation into coupled one-dimensional equations, which are then solved using the Flux-Corrected Transport (FCT) algorithm of Boris and Book. Non-reacting materials are described using either a perfect gas, Mie-Gruneisen, or Tait equation of state, while the energetic materials are described using either a BKW equation of state and Forest Fire reaction rate model, or the JWL equation of state and the Ignition and Growth reaction rate model. A modified Young's algorithm is used to maintain a sharp interface between different materials on the computational mesh. A brief description of the major components of the coding is provided, and then several applications of the code are described, including the simulation of bullet impact experiments, the underwater sympathetic detonation test, and the modified gap test.

RELEASE LIMITATION

Approved for public release

1 9 9 9 0 3 0 8 1 9 8

DEPARTMENT OF DEFENCE

DEFENCE SCIENCE AND TECHNOLOGY ORGANISATION

DTIC QUALITY INSPECTED 1

AQ F 99-06-1108

Published by

*DSTO Aeronautical and Maritime Research Laboratory
PO Box 4331
Melbourne Victoria 3001 Australia*

Telephone: (03) 9626 7000

Fax: (03) 9626 7999

© Commonwealth of Australia 1998

AR-010-605

August 1998

APPROVED FOR PUBLIC RELEASE

Numerical Simulation of Detonation in Condensed Phase Explosives

Executive Summary

The ability to numerically simulate the propagation or failure of detonation in a variety of gaseous and condensed phase explosives is of fundamental interest to the military community. Much of the work of the DSTO is now done through computer simulation techniques, and hydrocodes are the favoured method for modelling warhead outputs and their effects on targets. Enhancing the capabilities of our hydrocodes directly enhances our ability to provide better advice to the Australian Defence Force in the areas of airblast, missile defeat, fragmentation, and the defeat of fixed or mobile land targets. Hydrocodes containing advanced energetic reaction rate models are also used to model safety related aspects of weapons such as sympathetic detonation, cookoff, and bullet and fragment impact. The work described here has provided WSD with a sophisticated hydrocode which can be used to provide an in-house capability to model non-standard explosive/shock interaction problems.

In this report we describe the development of an in-house two-dimensional multi-material Eulerian hydrocode to model the effects of detonating condensed phase explosives on surrounding materials. The code has the capability to model standard military explosives, which have so called ideal detonation behaviour, as well as the newer underwater military explosives which display highly non-ideal behaviour. The code has been designed to provide DSTO personnel involved in the modelling of energetic materials response with an in-house hydrocode capability which can be quickly adapted to model novel materials in non-standard environments for which current commercial hydrocodes may not be appropriate.

The code solves a set of equations describing the conservation of mass, momentum, and energy for an inviscid, compressible fluid. A computational technique known as operator splitting is used to reduce the two-dimensional calculation into sets of coupled one-dimensional equations, which are then solved using the Flux-Corrected Transport (FCT) algorithm of Boris and Book. Non-reacting materials are described using either a perfect gas, Mie-Gruneisen, or Tait equation of state. Ideal explosives are described using either a BKW equation of state and Forest Fire reaction rate model, or the JWL equation of state and the Ignition and Growth reaction rate model. A programmed burn option is also available, which forces the explosive to detonate at the correct detonation velocity and pressure. A model for non-ideal explosives is also included. This uses a three term reaction rate model developed for composite explosives, and a polytropic equation of state with a density dependent index.

The code described here is an Eulerian code, which means that the computational grid is fixed in space and different materials in the simulation flow through the grid at different rates. Maintaining a sharp interface between different materials is a common problem in Eulerian codes, and the problem is solved here by using a modified Young's algorithm to prevent numerical diffusion from smearing the interface between different materials on the computational mesh. This is a two-dimensional scheme in which an interface between two different materials within a cell is approximated by a straight line.

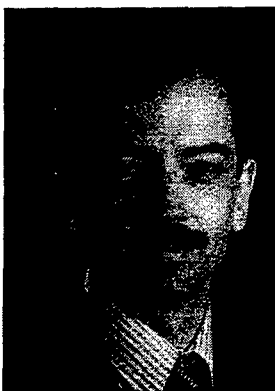
Authors



D.A. Jones

Maritime Platforms Division

David Jones graduated from Monash University in 1972 with a BSc (Hons). He obtained his PhD from Monash in 1976. His thesis was titled "Anisotropic diffusion in the Townsend-Huxley experiment". After working at Strathclyde University, London University and the University of New South Wales he joined AMRL in 1983. He has worked on the numerical modelling of shaped charge warheads and slapper detonator devices. From February 1987 to May 1988 he was a Visiting Scientist at the Laboratory for Computational Physics and Fluid Dynamics at the Naval Research Laboratories in Washington DC. While there he worked on advanced computational fluid dynamics.



G. Kemister

Air Operations Division

Gary Kemister graduated from Sydney University in 1980 with a B.Sc (Hons I) and in 1985 with a Ph.D in theoretical chemistry. After working at Oxford University, University of North Carolina at Chapel Hill, Sydney University and La Trobe University on various aspects of electronic structure of materials he joined the Defence Department in 1991 working for the Analytical Studies Unit in Force Development and Analysis Division in Canberra. In 1993 he moved to Explosive Ordnance Division (now part of Weapons Systems Division) at Maribyrnong where he worked on numerical simulations of the physics and chemistry of explosions. In February 1997 he moved to Air Operations Division.



R.A.J. Borg

KODAK, Australia

Rodney Borg graduated from the University of Melbourne with a B.Sc (Hons) in Chemistry in 1987. He joined the then MRL in 1988 and undertook a Ph.D. from Flinders University in Physical Chemistry in 1993. Since then he has worked on various experimental and theoretical projects with high explosives. He left AMRL in February 1996 to work with Kodak.

Contents

1. INTRODUCTION	1
2. HYDRODYNAMIC FLOW EQUATIONS.....	2
2.1 Transport Equations	2
2.2 Equations of state for non-reactive materials.....	3
3. IDEAL EXPLOSIVES	4
3.1 The HOM Equation of state.....	4
3.2 The JWL Equation of state	5
3.3 Reaction rate models	6
3.3.1 Forest Fire.....	6
3.3.2 Ignition and Growth.....	7
3.3.3 Programmed Burn	8
4. NON-IDEAL EXPLOSIVES.....	9
4.1 Introduction	9
4.2 Reaction rate scheme.....	10
5. NUMERICAL SOLUTION	11
5.1 Introduction	11
5.2 Program MULTI.....	14
5.3 Time Step Control.....	15
6. REPRESENTATIVE RESULTS	16
6.1 Bullet impact simulations	16
6.2 Underwater Sensitivity Test Simulation.....	17
6.3 Modified Gap Test Simulation	23
7. DISCUSSION AND CONCLUSION.....	27
8. ACKNOWLEDGMENTS	28
9. REFERENCES.....	29

1. Introduction

The ability to numerically simulate the propagation or failure of detonation in a variety of gaseous and condensed phase explosives is of fundamental interest to the military community. Computer codes which allow these calculations to be performed in a routine manner were developed during the 1960's and 1970's, and many of these codes have now been released to the general defence community. The codes developed by Mader at the Los Alamos National Laboratory to model detonation in condensed phase explosives include the Lagrangian finite difference codes SIN [1] and 2DL [2], as well as the multimaterial Eulerian codes 2DE [3] and 3DE [4]. An extensive review of the theory and equations used in these codes has been given in the monograph by Mader [5]. Other codes have been developed which concentrate primarily on material deformation and unreactive shocks, and these include the HELP code of Hageman and Walsh [6], the HULL code [7], and the DYNA2D code of Hallquist [8]. These codes contain only a rudimentary treatment of the physics of detonation when compared with Mader's codes, although recent versions of DYNA2D have included the Lee and Tarver Ignition and Growth model for the development of detonation in condensed phase explosives .

Over the past 12 years Weapons Systems Division has acquired most of these codes and applied them to a variety of explosive/material interaction problems. These have included the use of HELP to model jet formation in the MRL 38 mm shaped charge [9], the use of SIN and 2DL to model the propagation of detonation in ladder fracture tape [10], and the application of DYNA2D to model liner deformation in a variety of explosively formed projectiles [11-14]. While these examples have been notable successes, there have also been problems when codes have been applied to situations for which they were initially unsuited. Lack of documentation regarding the inner working of the codes has also often caused problems, and the large size of some of these multipurpose codes has also been a disadvantage when codes have had to be migrated between different computing systems.

To overcome some of these problems WSD has been developing in-house reactive Eulerian hydrocodes using the Flux-Corrected Transport (FCT) algorithm of Boris and Book [15,16]. Early work centred on the development of a multi-species code to model detonation transfer in gaseous explosives [17-19], and the development of codes to model shock propagation in elastic-plastic materials [20, 21]. More recent applications of these codes have included the modelling of detonation initiation and failure in gaseous systems [22-26], and air blast problems associated with explosive breaching operations [27-31]. The codes have recently been considerably extended by the addition of advanced interface tracking algorithms [32,33], enhanced graphics capabilities [34], and the inclusion of algorithms to model detonation in condensed phase explosives [35].

The code development described above has resulted in the production of an in-house 2D multi-material reactive Eulerian hydrocode (known as MULTI), which has recently been used to model several explosive/material interaction problems concerned with explosive sensitivity and safety [36, 37]. In this report we describe the basic features of

the MULTI code and give examples of its application to several standard detonation problems. MULTI has the capability to model standard military explosives, which have so called ideal detonation behaviour, as well as the newer underwater military explosives which display highly non-ideal behaviour.

In the next section we describe the basic hydrodynamic transport equations which govern the propagation of shocks in both reactive and non reactive materials. In section 3 we discuss the modelling of ideal explosives and describe their behaviour using both the Becker-Kistiakowsky-Wilson (BKW) equation of state and the Forest Fire reaction rate model, as well as the Jones-Wilkins-Lee (JWL) equation of state and the Ignition and Growth reaction rate model. In section 4 we consider non-ideal explosives and describe a model for the reaction rate and equation of state of a typical underwater explosive, PBXN-111. The numerical solution of the coupled set of equations describing hydrodynamic flow and chemical reaction is described in section 5. We first briefly discuss the development of MULTI, and then give a broad outline of the function of each of the various files and subroutines which are contained in the code, as well as an explanation of the input data file. In section 6 we describe the results of the code when used to simulate typical problems for both ideal and non-ideal explosives, and in section 7 we provide a summary of the code capabilities and areas of application.

2. HYDRODYNAMIC FLOW EQUATIONS

2.1 Transport Equations

Detonation phenomena occur on the microsecond time scale, and it is usual to assume that energy transport by heat conduction, viscosity, and radiation is negligibly small compared with transport by motion. The pressures generated by the detonation of a condensed phase explosive are of the order of 10^5 atmospheres. Under these conditions the strength of any confining material is completely negligible, and the material responds hydrodynamically. In this case, the appropriate equations which describe the material response are the Euler equations, which describe the conservation of mass, momentum and energy for an inviscid, compressible fluid. These have the following form [16]:

$$\frac{\partial \rho}{\partial t} + \nabla \cdot (\rho \mathbf{v}) = 0 \quad (1)$$

$$\frac{\partial (\rho \mathbf{v})}{\partial t} + \nabla \cdot (\rho \mathbf{v} \mathbf{v}) = -\nabla P \quad (2)$$

$$\frac{\partial E}{\partial t} + \nabla \cdot (E \mathbf{v}) = -\nabla \cdot (P \mathbf{v}) \quad (3)$$

In equations (1) - (3), ρ is the density, \mathbf{v} the fluid velocity, P the hydrodynamic pressure, and E the total energy per unit volume, which is given by the following expression

$$E = \rho e + 0.5\rho v^2 \quad (4)$$

where e is the specific internal energy.

The above equations are supplemented by both a mechanical equation of state for the pressure and a caloric equation of state for the temperature, which have the form

$$P = P(\rho, e, \lambda) \quad (5)$$

$$T = T(\rho, e, \lambda) \quad (6)$$

where T is the temperature and λ is the explosive mass fraction. The equations are then closed by specifying an expression for the rate of change of λ . The exact form of this expression depends on the details of the explosive decomposition reaction, and for the moment we simply write

$$\frac{d\lambda}{dt} = f(P, e, \lambda) \quad (7)$$

When the reaction occurs in a fluid moving with a velocity v the time derivative in equation (7) denotes a derivative following the fluid flow, and equation (7) becomes

$$\frac{\partial \lambda}{\partial t} + v \cdot \nabla \lambda = f(P, e, \lambda) \quad (8)$$

Equation (8) can then be combined with equation (1) so that the equation describing chemical reaction in the moving fluid can be written in the form

$$\frac{\partial(\rho\lambda)}{\partial t} + \nabla \cdot (\rho\lambda v) = f(P, e, \lambda) \quad (9)$$

Equation (9) then has the same form as equations (1) through (3) and can be solved by the same numerical technique.

The numerical solution of the progress of the detonation therefore requires the solution of equations (1), (2), (3), which describe conservation of mass, momentum and energy respectively, together with the solution of the equations of state given by equations (5) and (6), and the equation describing the rate of reaction, equation (9). The numerical techniques used to solve these equations will be described in section 5. In the next few sections we discuss appropriate equations of state which are used to describe the behaviour of both non-energetic and reactive materials.

2.2 Equations of state for non-reactive materials

The most commonly used equation of state for condensed phase materials is the Mie-Grüneisen equation of state, which has the form [38]:

$$P = P_H + \gamma(e - e_H)\rho \quad (10)$$

where P_H and e_H refer to the pressure and specific internal energy along the shock compression curve, known as the Hugoniot, and which have the form

$$P_H = P_o + \rho_o c_o^2 \eta / (1 - s_o \eta)^2 \quad (11)$$

$$e_H = e_o + 0.5(P_H + P_o)\eta / \rho_o \quad (12)$$

where η is the compression, defined by $\eta = 1 - \rho_o/\rho$, and c_o is the sound speed in the undisturbed material. In the above expressions the shock velocity u_s and the particle velocity u_p are assumed to obey a linear relationship of the form $u_s = c_o + s_o u_p$. The constant γ is known as the Gruneisen gamma, and the product $\gamma\rho$ is assumed to be a constant, and is given by the expression

$$\gamma\rho = 3\alpha / (C_v K) \quad (13)$$

where α is the coefficient of linear thermal expansion, K is the isothermal compressibility, and C_v is the specific heat at constant volume.

Equation (10) effectively describes the hydrodynamic shock response of many materials, including metals, unreacted explosives, and water. In the case of water however a simpler equation of state, the Tait equation [39], is sometimes used. This has the form

$$\frac{p}{p_o} = \left(\frac{B}{\rho_o}\right) \left[\left(\frac{\rho}{\rho_o}\right)^n - 1 \right] + 1 \text{ for } \frac{\rho}{\rho_o} \geq 1 \quad (14)$$

$$\frac{p}{p_o} = \left(\frac{\rho}{\rho_o}\right)^m \text{ for } \frac{\rho}{\rho_o} < 1 \quad (15)$$

where p_o and ρ_o are pressure and density at standard conditions, taken as 1 atm and 1000 kg/m³, respectively. The quantities B , n , and m are constants which have the values 3010 atm, 7.14, and 21457.15 respectively [40].

3. IDEAL EXPLOSIVES

3.1 The HOM Equation of state

Energetic materials require different equations of state to describe the condensed phase material before detonation, and the gaseous detonation products after reaction. The HOM Equation of State (EOS) uses the Mie-Gruneisen EOS to describe the unreacted material, while the BKW EOS is used to describe the highly non-ideal gaseous products after reaction. For a mixture of gases the BKW EOS has the form [5]:

$$P_g V_g / (RT) = 1 + x \exp(\beta x) \quad (16)$$

where $x = k/[v_g(T+\theta)^\alpha]$ and k is the average covolume defined in terms of the individual covolumes k_i as $k = \kappa \sum x_i k_i$, where x_i is the mole fraction of species i . The α ,

β , κ , and θ are constants adjusted to reproduce the detonation pressure and velocity obtained experimentally.

By using various thermodynamic expressions equation (16) can be used to construct the free energy for a given composition, and then the equilibrium composition can be determined by minimizing the free energy with respect to the molar fractions. This procedure is described in detail in the monograph by Mader [5], and in a recent DSTO report [41]. To avoid performing this calculation every time the equation of state of the products is needed in a hydrocode calculation however it is assumed that the states encountered in a typical calculation are close to those on the equilibrium isentrope through the CJ point. Mader has used his BKW code to fit the equilibrium isentrope through the CJ point for many different explosives to a set of polynomials of the form

$$\ln P_i = A + B(\ln v_g) + C(\ln v_g)^2 + D(\ln v_g)^3 + E(\ln v_g)^4 \quad (17)$$

$$\ln \varepsilon_i' = K + L(\ln P_i) + M(\ln P_i)^2 + N(\ln P_i)^3 + O(\ln P_i)^4 \quad (18)$$

$$\ln T_i = Q + R(\ln v_g) + S(\ln v_g)^2 + T(\ln v_g)^3 + U(\ln v_g)^4 \quad (19)$$

where v_g is the specific volume of the detonation products, the shifted internal energy $\varepsilon_i' = \varepsilon_i + Z$, and Z is a constant used to change the standard state to be consistent with the condensed explosive one. In a hydrocode calculation then the BKW equation of state for the reaction products is approximated by an equation of Mie Gruneisen form, where the reference state is now the isentrope through the CJ point, rather than the Hugoniot, ie.

$$P_g = P_i + \gamma \rho (e_g - e_i) \quad (20)$$

where the subscripts i and g refer to the isentrope and the gaseous products, and γ is now the Gruneisen gamma for the detonation products.

3.2 The JWL Equation of state

The Jones-Wilkins-Lee equation of state has been used extensively to describe the behaviour of the detonation products of explosives in contact with metal casings. It has the form [42]:

$$p = A\left(1 - \frac{\omega}{R_1 V}\right) \exp(-R_1 V) + B\left(1 - \frac{\omega}{R_2 V}\right) \exp(-R_2 V) + \frac{\omega E}{V} \quad (21)$$

where p is the pressure in megabars. V and E are given by $V = \rho_o/\rho$ and $E = \rho_o e$, and A , B , R_1 , R_2 , and ω are constants for a particular explosive. The JWL constants are derived by a trial and error procedure in which the expansion record in a standard cylinder expansion test is simulated using a hydrocode, usually DYNA2D, and the constants are varied until the simulated expansion record matches the experimental data. Values for these constants can be found in a variety of sources, including Dobratz and Crawford [43], and Karpp [44]. Equation (21) can also be used to describe the equation of state of unreacted explosives [51].

3.3 Reaction rate models

The shock initiation of a condensed phase heterogeneous explosive is a complicated process which is still not completely understood. Most condensed phase explosives consist of poly crystalline materials containing voids of various shapes and sizes, defect structures, and often small amounts of polymeric binders and plasticisers. When a shock wave travels through such material it provides heating both by bulk compression and by the interaction of the shock with the various density discontinuities and defect structures. The localised regions of high temperature caused by these density discontinuities are known as hot spots, and if conditions are favourable these hot spots may begin to react and lead to the formation of a stable detonation, even though the temperature rise caused by the bulk heating may be insufficient by itself to lead to detonation. Current understanding of the initiation of detonation of heterogeneous explosives by shock therefore divides the process into two distinct stages:

- (i) Ignition of a small fraction of the explosive at random sites within the sample due to the creation of hot spots.
- (ii) Growth to detonation from the coalescence of the energy released from the individual hot spots.

To numerically simulate the shock initiation of a condensed phase explosive we therefore need to find appropriate models for both the ignition and growth stages, and then combine these into an appropriate equation for the overall rate of explosive decomposition. Many models for hot spot formation have been derived, and many different reaction rate schemes have been proposed. A critical review of some of these reaction rate schemes can be found in the report by Jones [45]. The MULTI code currently contains the Forest Fire, Ignition and Growth, and CPEX (Commercial Performance of Explosives) reaction rate models, although additional reaction rate models could be implemented with relative ease.

3.3.1 Forest Fire

The Forest Fire model was one of the first reaction rate schemes used to characterise the decomposition of a heterogeneous explosive. It was first described by Mader and Forest [46], and a good description of the model can be found in the monograph by Mader [5]. It is a purely phenomenological model and assumes that the reaction rate can be expressed as a power series in pressure, and therefore has the form:

$$\frac{d\lambda}{dt} = (1 - \lambda) \exp\left(\sum_{i=0}^{i=14} a_i P^i\right) \quad (22)$$

where λ represents the fraction of reacted explosive. The finite rate of burning expressed by equation (22) yields a reaction zone of finite thickness in which λ varies between 0 and 1, and which contains a mixture of condensed explosive and gaseous products. In such regions thermal and mechanical equilibrium between the two phases

of the explosive are used and an iterative technique is used to determine the specific internal energy of each phase.

Wedge test data has been traditionally used to obtain the coefficients in equation (22). In this test a wedge of high explosive is placed in front of a planar shock wave generator and the distance that the shock runs through the wedge before detonation occurs is observed with a streak camera. In an ideal explosive the change to detonation is marked by a rapid change in shock velocity and is easily observed. By varying the initial shock pressure in the plane wave generator a plot can be made of the run distance to detonation as a function of the initial sustained shock pressure. Such a plot is known as a Pop plot, after its originator A. Popolato [47]. The Forest Fire coefficients are then obtained by fitting to the Pop plot data. In order to perform this fit several assumptions have to be made, and the validity of these assumptions have been analyzed recently by Starkenberg [48], Lundstrum [49], and Liang et al. [50]. Although some of the assumptions regarding the flow behind the shock front are overly simplistic, it appears that replacing these assumptions with more realistic expressions has little effect on the computed coefficients. Because of the relative ease in conducting the wedge test, and also in fitting the Forest Fire coefficients to the Pop plot data, it is fairly easy to obtain the Forest Fire coefficients for a number of ideal military explosives. Mader [5] contains a comprehensive listing of these.

3.3.2 Ignition and Growth

The original Lee and Tarver model [51] divided the initiation process into two distinct stages. In the first stage, the ignition stage, the passage of the shock front creates hotspots at density discontinuities within the heterogeneous material. In the second stage, the growth stage, the hot spots are assumed to grow by a grain burning process until they eventually coalesce to form a stable detonation. The model is phenomenological in the sense that plausible assumptions are made regarding the physical mechanisms for each of these stages, and then a generalised energy release rate of the following form is considered:

$$\frac{\partial \lambda}{\partial t} = I(1 - \lambda)^x \eta^r + G(1 - \lambda)^x \lambda^y p^z, \quad (23)$$

$$\eta = V_0 / V_1 - 1, \quad (24)$$

where λ is the fraction of explosive that has reacted, V_0 is the initial specific volume of the explosive, V_1 is the specific volume of the shocked, unreacted explosive, and I , x , r , G , y and z are constants.

Different hot spot models lead to different values for the constant r . If the ignition rate is assumed to be proportional to the strain rate in the shocked explosive then $r = 1$. If the hot spots are formed by the stagnation of micro jets model then $r = 3$, while if the hot spot model is based on the amount of plastic work done during void collapse then $r = 4$. Best overall agreement with experiment has been found using $r = 4$.

The constants x and y are related to the choice of the geometry for the hot spot combustion process. Hot spots can be considered to burn outwards from the void centre, or inward over the total grain surface. Lee and Tarver considered a spherical hot spot burning outward, which corresponds to $y = 2/3$. Requiring that the rate be a maximum when the combustion surfaces overlap leads to the value $x = 2/9$.

The remaining constants I , G and z are found by combining equation (23) with the JWL equation of state (for both the reacted and unreacted explosive), implementing the scheme in a Lagrangian hydrocode (DYNA2D), and then fitting simulated pressure-time records to experimentally measured embedded gage records. In their original publication Lee and Tarver applied the model to the explosives PBX-9404, TATB, PETN and cast TNT, and found that they were able to obtain good agreement with a variety of experimental data for explosives subjected to sustained shock loading. For short pulse duration shock initiation experiments however the model needs to be modified by the addition of an extra growth term before good agreement with experiment is obtained. Only the original two term Ignition and Growth model is implemented in MULTI, but the three term model is explained in Tarver et al. [52], and could easily be added to the code.

Embedded gauge experiments are fairly costly to conduct however and so relatively few explosives have been fitted to this model. Murphy et al. [53] have addressed this question and shown that it is possible to find ignition and growth parameters for Composition B by using a combination of existing data from standard tests for the material and extrapolation of the remaining unknown parameters from similar known explosives. Simulations of the wedge test and failure diameter tests were found to be sufficient to define the ignition and growth parameters used in the two term version of the reaction rate model. The coefficients were then used to model the response of several two-dimensional Composition B impact initiation experiments, and good agreement with the experimental data was found.

Miller [54] has also considered the problem of determining the reactive rate parameters for the ignition and growth model. His simplified ignition and growth model (SIG) consists of only two adjustable parameters, the ignition (I) and growth (G) rate constants, which are determined from experimental data on failure diameter and gap test sensitivity. Miller has applied his SIG model to four quite different explosives, PBXN-110, PBXN-111, PBXW-126 and PBX 9404, and found that there was very good agreement between simulated and observed embedded gauge stress-time profiles for each of these explosives.

3.3.3 Programmed Burn

A programmed burn is used in a hydrocode to simulate the detonation of an explosive when the properties of that particular explosive are well known, and it's behaviour is not the focus of the investigation. For example, a programmed burn could be used to detonate a charge in an air burst calculation when the effect of the air shock on specified targets was the main concern. In this particular application the characteristics of the explosive are well known and the programmed burn provides a simple and

robust method of ensuring the correct detonation pressure at the explosive/air interface.

In a programmed burn the basic assumption is that the detonation wave front travels in all directions at the Chapman-Jouguet detonation velocity. Information concerning the energy released from the explosive such as the burn time (BT) and burn interval (BI) are precalculated and stored in the code at time $t = 0$. For example, if the initiation point of the detonation is at x_d , then the arrival time of the detonation at a typical computational cell centre $x_{i+1/2}$ is given by

$$BT(i) = |x_{i+1/2} - x_d|/D \quad (25)$$

where D is the detonation velocity. During the calculation, when the cycle time t^n is greater than the burn time BT for a particular cell, but less than the time $(BT + BI)$, then a fraction of the specific energy for that particular explosive is deposited into the cell. On each successive cycle this process is repeated until the cycle time is greater than $(BT + BI)$. The fraction of specific energy deposited each time is given by $(t^{n+1} - t^n)/BI$, and the burn interval BI is chosen so that the reaction zone is spread over several computational cells. In this way the correct C-J pressure, density and velocity can be imposed, and the resulting detonation front is guaranteed to have the correct profile.

4. NON-IDEAL EXPLOSIVES

4.1 Introduction

All explosives exhibit some form of diameter effect in which the detonation velocity decreases with decreasing charge diameter until a critical diameter is reached and stable detonation cannot be sustained. For ideal explosives the change in velocity with diameter is minimal until very close to the critical diameter, whereas for non-ideal explosives the diameter dependence is very pronounced and the velocity at the critical diameter can be as low as 30% of the value at infinite diameter. Non-ideal explosives contain separate fuel and oxidizer species, often in physically separated phases, and their heterogeneous nature leads to much larger reaction zone lengths and more curved detonation fronts than those in ideal explosives.

The analysis of non-ideal explosives is considerably more involved than that of ideal explosives, and has only begun to be addressed in the context of military explosives during the last few years. Reaction rate schemes such as Forest Fire and Ignition and Growth were designed for ideal military explosives, and have been very successful in modelling the performance of these types of explosives. Their applicability to non-ideal explosives is still uncertain however, although recent progress in this area has been made by Miller [54], and Miller and Sutherland [55].

Underwater explosives typically display highly non-ideal behaviour, and one such explosive which has been of considerable interest in recent years is PBXN-111

(formerly known as PBXW-115), which has the formulation 20% RDX, 43% ammonium perchlorate, 25% aluminium, and 12% HTPB binder. Kennedy and Jones [56] have analysed the detonics of this underwater explosive using small divergent detonation theory, and by calibrating a reaction rate model to experimental detonation velocity measurements as a function of charge diameter. The model was implemented in the finite element hydrocode DYNA2D, which was then used to simulate a variety of initiation and detonation tests, and the results were generally in excellent agreement with the experimental data. The model has since been included in the MULTI code, and the next section briefly describes the model as implemented in MULTI.

4.2 Reaction rate scheme

The reaction rate used to model PBXN-111 was developed for composite explosives by Kirby and Leiper [57] and has the form

$$\frac{d\lambda}{dt} = (1-\lambda) \left[\frac{p_{hs} a_h}{\tau_h} + \frac{p a_i}{\tau_i} + \frac{p a_f}{\tau_f} \right], \quad (26)$$

where

$$p_{hs} = \frac{p}{4} \left(\frac{3p}{4p_{cr}} \right)^3 \quad \text{for } p < 4p_{cr}/3 \quad (27)$$

and

$$p_{hs} = p - p_{cr} \quad \text{for } p \geq 4p_{cr}/3 \quad (28)$$

λ is the progress variable which describes the extent of reaction, and varies from 0 for unreacted explosive to 1 for detonation products. The subscripts are: h for hotspot, i for intermediate, and f for the final stages of the reaction. There are four adjustable parameters; three characteristic reaction times τ , and the critical pressure p_{cr} that inhibits the onset of the hotspot reaction. The a_i are Gaussian form functions which describe the assumed geometry of the burn front and which switch the reactions on and off as the various phases are ignited and consumed. The a_i depend on λ and the initial formulation of the explosive as follows:

$$\begin{aligned} a_h &= \exp\{-(\lambda - C_i)/W_h\}^2 & \text{for } 0 \leq \lambda \leq C_i \\ a_h &= \exp\{-(\lambda - C_i)/W_i\}^2 & \text{for } C_i \leq \lambda \leq 1 \end{aligned} \quad (29)$$

$$\begin{aligned} a_i &= 0 & \text{for } 0 \leq \lambda \leq C_i \\ a_i &= 1 - a_h & \text{for } C_i \leq \lambda \leq C_f \\ a_i &= \exp\{-(\lambda - C_i)/W_h\}^2 & \text{for } C_f \leq \lambda \leq 1 \end{aligned} \quad (30)$$

$$\begin{aligned} a_f &= 0 & \text{for } 0 \leq \lambda \leq C_f \\ a_f &= 1 - a_h - a_i & \text{for } C_f \leq \lambda \leq 1 \end{aligned} \quad (31)$$

The Gaussian parameters are defined in terms of the mass fractions, Φ , of the three stages as:

$$\begin{aligned} C_i &= \Phi_h^2 \\ C_f &= (\Phi_h + \Phi_i)^2 \\ W_h &= 2C_i / (1 + C_i) \end{aligned} \quad (32)$$

$$\begin{aligned} W_i &= \Phi_h (1 - \Phi_h) \\ W_f &= \Phi_f (1 - \Phi_f) \end{aligned} \quad (33)$$

The equation of state of both the unreacted and reacted phases has a simple density dependent polytropic equation of the form

$$e = \frac{P}{\rho} (g - 1)^{-1} \quad (34)$$

where
$$g = g_0 + g_1 \rho + g_2 \rho^2 \quad (35)$$

The values of the constants g_i for the explosive products are found by fitting to isentrope data from an ideal thermodynamic code, while the constants for the unreacted phase are obtained by considering the shock data of the explosive and using known Hugoniot data. The unreacted solid state is usually a mixture of ingredients, and in this case the Hugoniot of the components are combined using the method of Afanasenkov et al. [58]. The equation of state for the partially reacted mixture is then completely specified by invoking the mixture rules

$$p = p_x = p_p, v = v_x = v_p, e = (1-\lambda)e_x + \lambda e_p \quad (36)$$

where the subscript x refers to the unreacted explosive, and the subscript p refers to the reacted, or product, phase.

5. NUMERICAL SOLUTION

5.1 Introduction

We have experimented with two slightly different approaches to the solution of the coupled equations described in the previous sections. In both cases operator splitting was used to decouple the transport stage from the chemical reaction stage, and then the two-dimensional transport equations were further decoupled into two sets of one-dimensional equations. This is a standard technique for the solution of coupled transport equations and is described in detail by Oran and Boris [16].

In the first version of the code the density of each material on the grid was convected independently by making repeated calls to the LCPFCT algorithm [59] for each material. The momentum flux and total energy flux (ie. specific internal energy plus

kinetic energy) for each material were then added and the combined fluxes convected using LCPFCT. This approach is illustrated in the equations listed below, which show the sequence of equations to be solved for the x-pass in a 2D cartesian grid calculation; ρ_i is the density of the i 'th material on the grid, ρu and ρv are the x and y components of the TOTAL momentum in each cell, and E is the TOTAL energy per unit volume in each cell.

$$\frac{\partial \rho_i}{\partial t} + \frac{\partial \rho_i u}{\partial x} = 0 \quad (37)$$

$$\frac{\partial \rho u}{\partial t} + \frac{\partial \rho u u}{\partial x} = - \frac{\partial P}{\partial x} \quad (38)$$

$$\frac{\partial \rho v}{\partial t} + \frac{\partial \rho v u}{\partial x} = 0 \quad (39)$$

$$\frac{\partial E}{\partial t} + \frac{\partial E u}{\partial x} = - \frac{\partial P u}{\partial x} \quad (40)$$

Because of the multimaterial capability of the code and the diffusive nature of all numerical transport schemes an interface tracking algorithm is required to maintain a sharp interface between different materials on the grid. In the first version of the code we used the Simple Line Interface Calculation (SLIC) scheme of Noh and Woodward [60]. SLIC is a one-dimensional alternating direction method for the geometric approximation of fluid interfaces. The scheme constructs a representation of the interface between two materials from the volume fractions of the materials in the mixed cell, and by testing whether or not the various fluids in the mixed cell are present or absent in the zone just to the left and to the right in the coordinate direction under consideration. The interface between two different materials is therefore represented by a number of one-dimensional components, each of which is composed entirely of straight lines either perpendicular or parallel to the coordinate direction under consideration. LCPFCT assumes that the different materials in a mixed cell are spread homogeneously throughout the cell, and hence would calculate an incorrect flux in a mixed cell. The SLIC algorithm determines the correct amount of material to be advected into and out of a mixed cell, and then the LCPFCT algorithm is modified by imposing a multiplicative area factor at the correct cell boundary for each material. Further details of this procedure can be found in the report by Milne and Carnegie [32].

Whilst the above scheme convects the density of each material on the grid independently, only the total energy in each cell is convected. In order to calculate a unique pressure in each mixed cell both the density and specific internal energy of each material in the cell must be known, and so a way of dividing the total internal energy in each cell between the component materials must be devised. To do this we assumed pressure equilibrium between the materials in the mixed cell (this is a common

assumption in multimaterial Eulerian codes) and used an iterative procedure to determine the internal energy of each component.

The above scheme was used in a variety of trial calculations, including both one-dimensional and two-dimension flying plate impact simulations, but problems were found to occur at the interface between different materials. In particular, whilst the average numerical values for the dynamical variables were accurately predicted, there were perturbations to both the velocity and pressure profiles in the vicinity of the interfaces.

These disturbances were traced to the way in which the total energy was convected, and to a discrepancy between the mass fluxes and interface velocities used in the partial density calculations, and the momentum fluxes used in the principle momentum component equation. These problems were eliminated by adding additional coding to convect the internal energy of each species separately, and by slightly rearranging the order of the transport equations. The advantage of following the internal energy of each material is that an iterative calculation is no longer needed in each mixed cell, and the pressure in the cell is determined from a simple volume average of the partial pressures within the cell. To ensure correct volume fluxes it was also decided to base the interface tracking calculations on a donor cell scheme rather than an FCT scheme. Hence in the later version of the code the fluxes for energy and density in a mixed cell are overwritten by a donor cell calculation.

The sequence of equations to be solved for the x-pass in a 2D cartesian grid calculation in this version of the code now have the form shown below, where ρ_i and e_i are the density and specific internal energy respectively of the i 'th material on the grid, and u and v are the x and y components of the velocity in each cell.

$$\frac{\partial \rho_i}{\partial t} + \frac{\partial \rho_i u}{\partial x} = 0 \quad (41)$$

$$\frac{\partial u}{\partial t} + \frac{\partial uu}{\partial x} = u \frac{\partial u}{\partial x} - \frac{\nabla P}{\rho} \quad (42)$$

$$\frac{\partial v}{\partial t} + \frac{\partial vu}{\partial x} = v \frac{\partial u}{\partial x} \quad (43)$$

$$\frac{\partial e_i}{\partial t} + \frac{\partial e_i u}{\partial x} = -P \frac{\partial u}{\partial x} \quad (44)$$

The current version of MULTI also uses an interface tracking algorithm based on Youngs method [61]. This is a two-dimensional algorithm which represents interfaces more accurately, as each portion of the interface in a cell is represented by a straight line. Simulation results on test problems using this new version of the code were found to be both more accurate and more robust, and hence only this version of the coding is described in detail in the following section.

5.2 Program MULTI

Program MULTI consists of a number of separate files, each of which will be described briefly here. The main driving program is contained in **multi.f**. This reads the input file **det.inp**, calls subroutine **INITAL**, which initialises all the variables, then calls subroutines **xtran.f** and **ytran.f**, which transport mass, momentum and energy in the X and Y directions respectively, and then calls subroutine **burn.f**, which models the decomposition of any explosive material on the grid. **multi.f** also includes function **SPEED**, and subroutines **MINTIME** and **TIMESTEP**, which allow the user to specify a variable time step for materials described by the HOM equation of state.

MULTI allows eight different material types, labelled by the index I, and characterised by a combination of several different equations of state and reaction rate laws. The eight different material types are listed below:

INDEX I	MATERIAL TYPE
1	Non reactive - Perfect Gas equation of state
2	Non reactive - Mie-Gruneisen equation of state
3	Reactive - Forest Fire reaction rate model and HOM equation of state
4	Reactive - Ignition and Growth reaction rate model and JWL equation of state
5	Reactive - an early version of JWL, now available for experimentation
6	Reactive - Programmed Burn reaction rate model and JWL equation of state
7	Non reactive - TAIT equation of state for water
8	Reactive - - CPEX burn model for non ideal explosives

multi.f first reads the input data file **det.inp** to determine the number of materials on the grid (NMAT), the type of boundary conditions (periodic or non-periodic), and the geometry, which is specified by **ALPHAX** and **ALPHAY**. **ALPHA = 1, 2 or 3** corresponds to planar, cylindrical, or spherical geometry, respectively, and **ALPHAX** and **ALPHAY** refer to the geometry in the X and Y directions. If the boundary conditions are non-periodic then they can be either reflective (R) or transmissive (T), and the boundary conditions at the extremes of the X and Y axes are specified by setting **BCL**, **BCR**, **BCB** and **BCT** to either R or T. The time step can be either fixed or variable, and this is specified by setting the logical variable **FIXED_TIME** to be either **.true.** or **.false.**. A variable time step is currently only allowed if the materials on the grid are described by either the perfect gas or HOM equations of state. **DELTA X** and **DELTA Y** specify the spatial cell sizes in the X and Y directions, and **NCX** and **NCY** specify the total number of cells in the X and Y directions.

det.inp then lists information about each of the materials on the grid, starting with the default material, which is automatically given the highest material number (equal to NMAT). The default material (for example, air, in an air blast calculation) is placed over the entire grid, and then other materials are placed at specific locations on the grid by specifying their minimum and maximum X and Y values (**IMIN**, **IMAX** and **JMIN**, **JMAX**). Each material requires specification of material type, initial density, initial velocity components U_0 and V_0 (for X and Y directions respectively) and **PRIORITY**. The priority value determines the order in which materials are convected from a mixed

cell. If the material is an explosive then the INITTYPE will be either 1 or 2, depending on whether a block of explosive (INITTYPE=1) or circle of explosive (INITTYPE=2) is to be placed on the grid. If a block of explosive is used then NDUMPX and NDUMPY specify a subsection of the explosive in which an additional amount of internal energy is added to initiate detonation. If a circular geometry is used then subroutine EXPLOSIVE_CIRCLE (file **mkcirc.f**) works out (from RADIUS, XCENTRE, and YCENTRE, which are specified in **det.inp**) which cells are full of explosive, and which cells have fractional amounts of explosive. Subroutine PUT_EXP_CIRCLE (file **put_circle.f**) then fills these cells with appropriate variable values. The circular explosive charge is initiated by compressing a smaller circular region. The radius of this region is typically half the radius of the full charge, and the explosive is compressed by calling subroutine PUT_HP_CIRCLE (file **put_hp_circle.f**) If a programmed burn is used instead to initiate the explosive then the compressive radius is set to zero.

The interface tracking part of the code is contained in files **fracvol.f**, **interfac.f**, and **choke.f**. **fracvol.f** is the basic interface tracking routine based on Youngs method [61]. **interfac.f** is used by **fracvol.f** to calculate mesh cell wall/interface intersections, and **choke.f** is an area factor which controls the amount of material advected across each cell interface. More information on these routines can be found in the report by Carnegie [33]. The file **press.f** contains the equation of state information and is called to calculate the pressure for each of the material types. Some of the equation of state coding is contained in files **jw1.f** and **hom1.f**, which are self-explanatory. **hom1.f** contains a simple addition to the HOM equation of state to ensure consistency with the perfect gas equation of state at low pressures. **burn.f** controls explosive burn. It contains subroutine CP_BURN, which describes the reactive rate law for non ideal explosives, and also calls **ffire.f** and **igburn.f**, which perform Mader's Forest Fire burn and the Lee and Tarver Ignition and Growth burn respectively. **lcpdc.f** is a version of **lcpfct.f** which solves partial density and energy equations assuming a donor cell scheme for mixed cells. **rtbis.f** is a real function which calculates roots of functions using the bisection method, and is used in several subroutines where pressure equilibrium is assumed.

5.3 Time Step Control

MULTI is an explicit finite difference code and hence the time step δt is limited by the Courant condition, which in one space dimension has the form [16]

$$\delta t \leq \min (\delta x / (|v| + c)) \quad (45)$$

where v is the particle velocity, c is the sound speed, and δx is the spatial cell size. Use of equation (45) ensures the stability of the coupled set of equations (1) - (3), (5) and (9). Expressions for the sound speed can be derived using standard thermodynamic arguments. For materials described by the HOM equation of state Guirguis and Oran [62] have derived expressions for the sound speed in the condensed phase, gas phase, and a mixture of both phases, and these expressions have been coded into MULTI so that simulations using only the HOM and perfect gas equations of state can be run

using a variable time step calculated from equation (45). If other equations of state are employed in the calculation then a fixed time step must be used.

6. REPRESENTATIVE RESULTS

6.1 Bullet impact simulations

MULTI has previously been used to simulate the impact sensitivity of the explosive Composition B, and detailed results can be found in the report by Borg and Jones [35]. The sensitivity tests used steel cylinders of varying diameters fired against Composition B to determine the critical impact velocity for initiation as a function of the projectile diameter. The experiments were later modelled by Starckenberg et al. [63] using Mader's 2DE code, and good agreement was found between the calculations and the experimental results. The MULTI calculations were undertaken partly as a validation exercise for the code. As the simulations were performed using Mader's HOM equation of state and the Forest Fire reaction rate scheme the MULTI results were expected to agree with Starckenberg's calculations, apart from any minor differences arising from the different transport algorithms and interface tracking routines in the codes.

The projectile impact calculations were performed using 2D cylindrical geometry and simulated the impact of a the cylindrical steel projectile onto a cylindrical Composition B explosive charge. Both the projectile and explosive charge were surrounded by air at atmospheric pressure. The air was described by a perfect gas equation of state, and the steel projectile by the Mie-Gruneisen equation of state.

The experiments determined the critical velocity (V_c), which is defined as the velocity of the projectile above which impact results in shock initiation, and below which the impact results in a lower order event such as a burn or deflagration. The critical velocity is a function of projectile diameter, and increases as the diameter of the projectile is reduced. Figure 1. shows a comparison between the simulated results calculated using MULTI, the experimental results of Slade and Dewey [64], and the 2DE computations of Starckenberg et al. [63]. The MULTI results are in close agreement with the calculations of Starckenberg et al., as expected. The discrepancy at larger projectile diameters can be explained by differences in the methods used to differentiate between a detonation and a fail in the two sets of calculations.

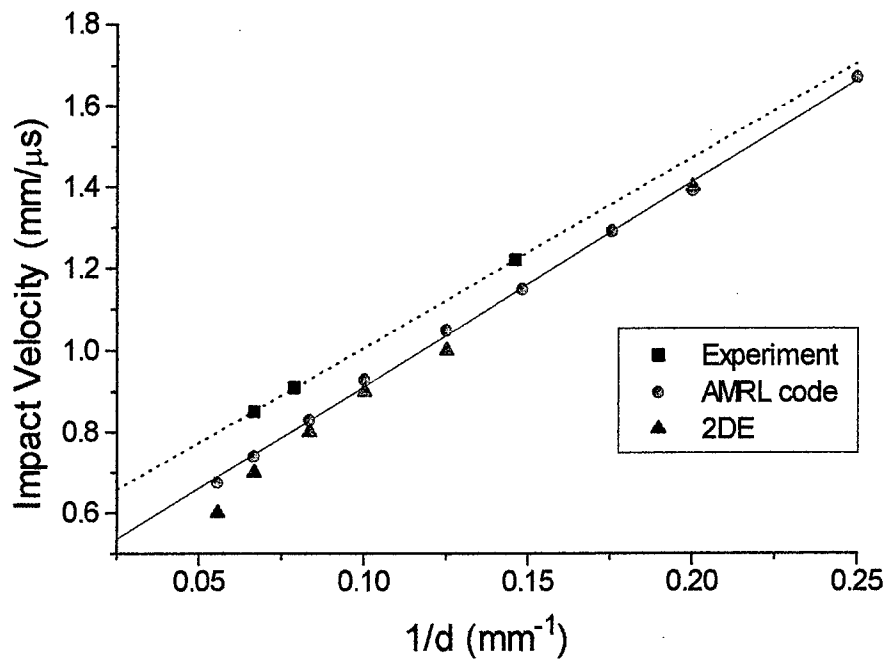


Figure 1: Plot of critical velocity as a function of inverse charge diameter for the MULTI simulations, the 2DE computations, and the experimental results.

6.2 Underwater Sensitivity Test Simulation

MULTI has recently been used to simulate the Underwater Sensitivity Test and Modified Gap Test for the explosive H-6 as part of a collaborative effort between the TTCF countries to validate national hydrocodes for the prediction of underwater sympathetic detonation. The US is the lead nation in this activity and proposed the numerical simulation of the underwater sensitivity of H-6 as a common benchmark problem, and has supplied each nation with extensive material and detonation property data on H-6. In this section we describe some of the recent Underwater Sensitivity Test calculations [37] to illustrate the application of MULTI to a typical problem.

The Underwater Sensitivity Test is described in detail by Liddiard and Forbes [65]. Figure 2 shows a schematic of the test assembly. A spherical pentolite donor is suspended in the aquarium and four acceptors, each cylindrical in shape, are spaced at varying distances around the donor with the flat surfaces facing the donor charge. The donor is an 82.2 mm diameter sphere of cast pentolite (50% TNT/50% PETN) weighing 470 - 480 g. The acceptors are 12.7 mm thick and have a diameter of 50.8 mm. Chemical reaction in the sample explosive is detected by measuring the expansion of the acceptor pellet after it is struck by the shock. If the axial length of the shocked acceptor, s , is plotted as a function of time, t , then usually a fairly constant rate of expansion, ds/dt ,

is obtained. The slope of the curve is then used to characterise the degree of reaction of the sample explosive.

The MULTI code was used to simulate the UST for several different donor - acceptor gap lengths. The simulations were run on a 160×160 grid in 2D cylindrical geometry with $\delta x = \delta y = 0.1$ cm and a fixed time step of $0.02 \mu s$. The detonation of the pentolite donor charge was modelled using a programmed burn algorithm, with a JWL equation of state] to describe the reaction products. For pentolite these have the values $A = 5.4094$, $B = 0.093726$, $R_1 = 4.5$, $R_2 = 1.1$, $\omega = 0.35$, and $E_0 = 0.081$. Initial density $\rho_0 = 1.70$ g/cm³, and $p_{cj} = 0.255$ Mbar. The pentolite data was taken from Dobratz and Crawford [43]. The water was modelled by the Tait equation of state, as described in section 2.2.

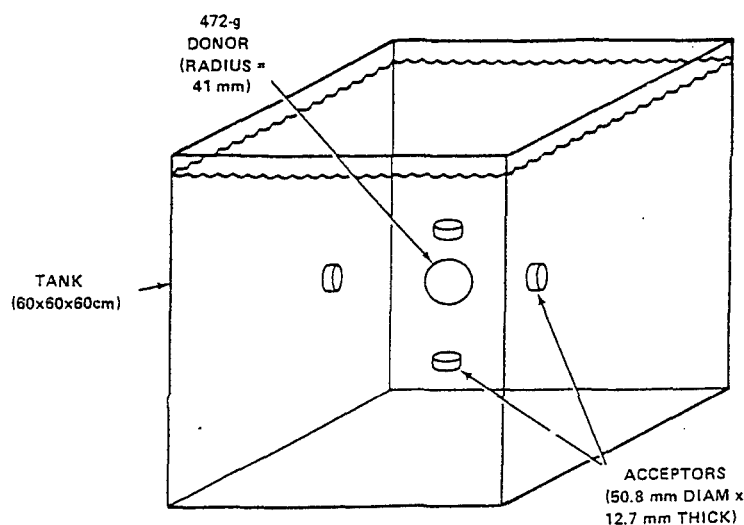


Figure 2: Schematic illustration of the Underwater Sensitivity Test.

The reactive model used for H-6 was derived by McIntosh and has been described in a recent publication [66]. The explosive decomposition is modelled by the Forest Fire reaction rate law and was calibrated using the experimental Pop Plot data reported by Hudson [67]. McIntosh used the JWL equation of state to model both the unreacted and reacted explosive material, and the DYNA finite element code was used to model both sensitivity tests. The calculations described here used the Forest Fire reaction rate law, but the HOM equation of state was used instead of JWL. The necessary constants were

provided by McIntosh [66]. Table 1 shows the input file **det.inp** for a typical MULTI run. In this case the donor - acceptor separation was 40 mm.

Before comparing simulated values with experimental results the accuracy of MULTI with respect to the shock pressure in water was checked. Figure 3 shows a comparison between the simulated pressure and the experimental pressure from the Underwater Sensitivity Test calibration reported by Liddiard and Forbes [65]. There is quite good agreement between the MULTI simulation and the NSW calibration for all the distances of interest.

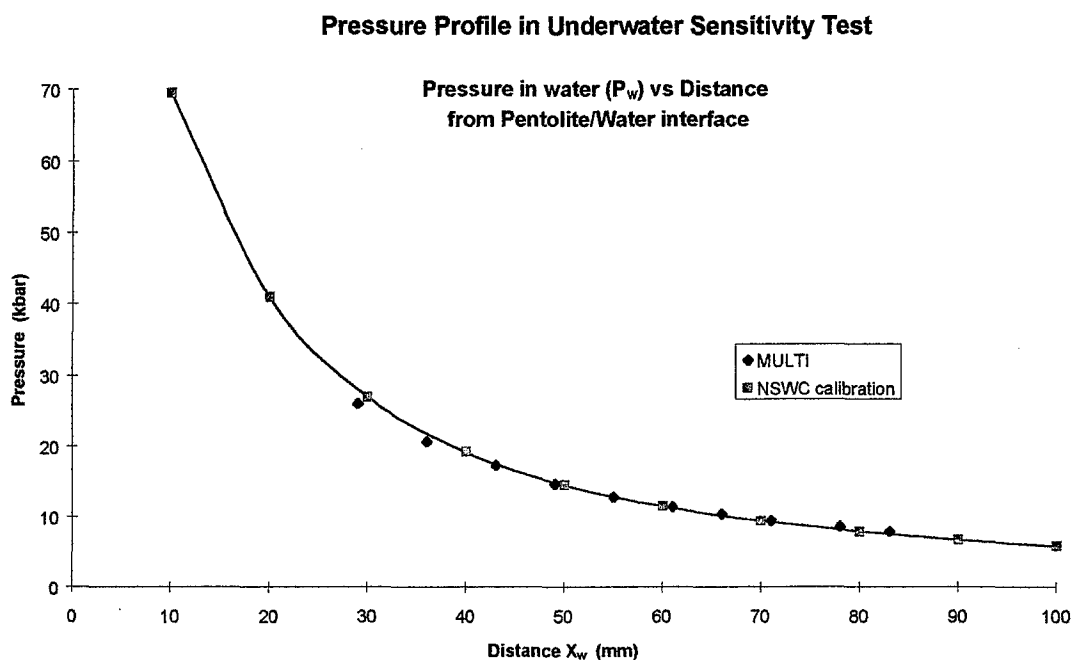


Figure 3. Shock pressure in the water gap of the UST as a function of distance from the surface of the pentolite donor.

Figures 4 and 5 show plots of the acceptor thickness as a function of time for water gap distances of 40 mm and 55 mm respectively. These show a fairly constant rate of expansion, and this is also found experimentally. The simulated ds/dt values are too high though; at 40 mm and 55 mm water gap distances the simulated values of ds/dt are 1.39 mm/ μ s and 0.92 mm/ μ s respectively, while the experimental values are 0.39 mm/ μ s and 0.38 mm/ μ s. These results are in agreement with the simulations of McIntosh however, who found that the simulations overestimated the velocities by factors of about two to three. This level of agreement with the DYNA results is to be expected as basically the same reactive model for H-6 has been used in both sets of calculations.

The rather poor level of agreement between the simulated results and the experimental results highlights an important point which should be considered in any reactive simulation; namely, the level of agreement will only be as good as the suitability of the reactive model used. Alternatively, if an appropriate reactive model is used, then the model should be calibrated to experimental data which is as close as possible in geometry, shock levels, etc., to the experimental data which is being simulated. The Forest Fire model for H-6 was calibrated to the wedge test data reported by Hudson [67]. Experimentally the wedge test has almost one-dimensional flow, while the UST is very much a two-dimensional test. Better agreement with the experimental results would have been obtained if the reactive model had been calibrated to experimental data exhibiting a strongly two-dimensional flow, such as some form of Gap Test data. This point is discussed in more detail in the paper by Jones [37].

Table 1: Input file det.inp for a typical MULTI run for the Underwater Sensitivity Test.

```

NMAT
3
PBC
0.0
ALPHAX
1
ALPHAY
2
BCL, BCR, BCB, BCT
'R', 'T', 'R', 'T'
DELTAX
0.100
DELTAY
0.100
DELTAT, FIXED_TIME
0.0200, .true.
NCX
160
NCY
160
DEFEOS, DEFC0, DEFGAMMA, DEFRHO, DEFTMP
7, 0.1483, 1.0, 1.0, 3.0E2
DEFU0, DEFV0, DEFPRORITY
0.0, 0.0, 3
INITTYPE, RADIUS
0, 0.0
XCENTRE, YCENTRE
0.0, 0.0
EOSTYPE(1), C0(1), GAMMA(1), RHO0(1), TMP0(1)
5, 0.0, 0.0, 1.70, 3.0E2
U0(1), V0(1), PRIORITY(1)
0.0, 0.0, 1
INITTYPE, RADIUS
2, 4.05
XCENTRE, YCENTRE
0.0, 0.0
IMIN(1), IMAX(1), JMIN(1), JMAX(1)

```

0, 0, 0, 0
ndumpx, ndumpy
0, 0
EOSTYPE(1), C0(1), GAMMA(1), RHO0(1), TMP0(1)
3, 0.0, 0.0, 1.760, 3.0E2
U0(1), V0(1), PRIORITY(1)
0.0, 0.0, 2
INITTYPE, RADIUS
0, 0.0
XCENTRE, YCENTRE
0.0, 0.0
IMIN(1), IMAX(1), JMIN(1), JMAX(1)
81, 94, 1, 25
ndumpx, ndumpy
0, 0
MINSTEP
1
MAXSTEP
3000
IPRINT
100
PMIN
0.0
FULLDONOR
.TRUE.
DUMP, RESTART
.FALSE., .FALSE.

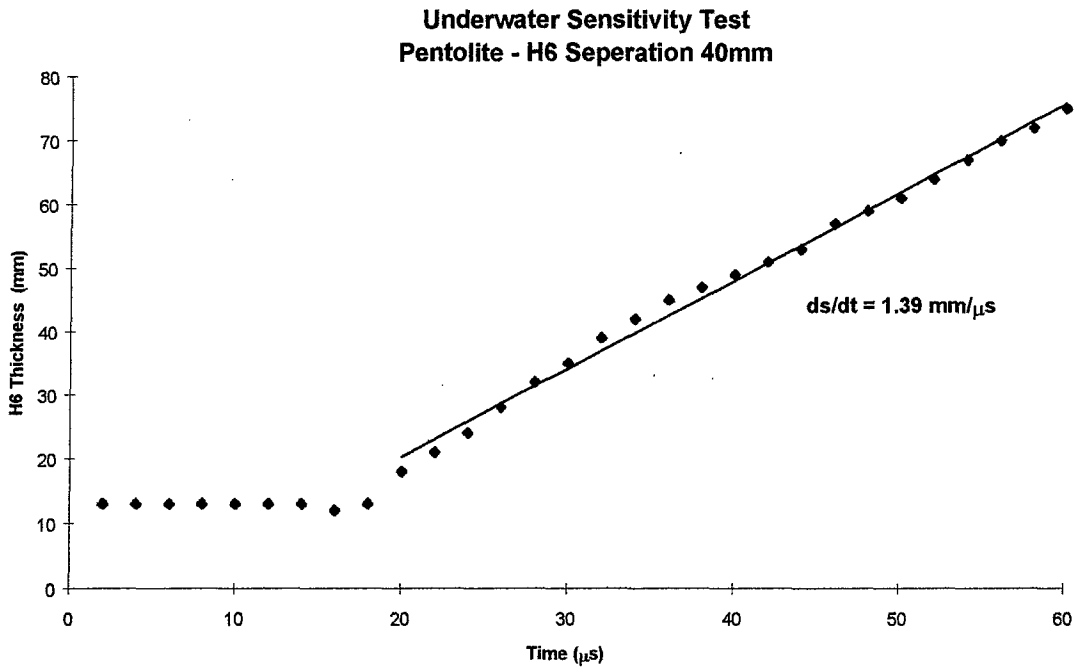


Figure 4. Plot of acceptor thickness as a function of time for a water gap of 40 mm.

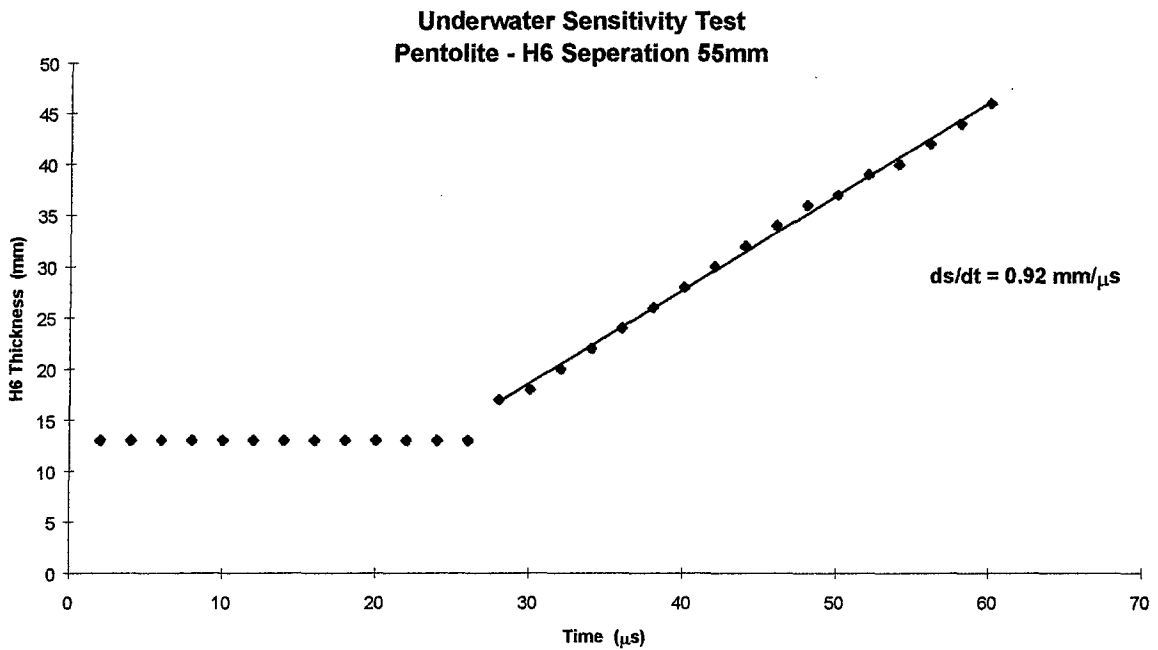


Figure 5. Plot of acceptor thickness as a function of time for a water gap of 55 mm.

6.3 Modified Gap Test Simulation

This section briefly describes the application of MULTI to the simulation of the Modified Gap Test for the TTCP collaborative hydrocode validation study on H-6 described in the previous section. The Modified Gap Test is described in detail by Liddiard and Forbes [65], and Figure 6 shows a schematic of the test assembly. It consists of a cylindrical donor explosive, a PMMA gap of variable length, and an acceptor explosive. The donor, gap, and acceptor are all 50.8 mm in diameter, and the donor for the H-6 acceptor runs was 50/50 pentolite. Figure 6 shows that two MGT set-ups are fired simultaneously to reduce costs, and a wooden baffle is used to prevent gases from the detonated donors from obscuring the view. The effect of the shock from the donor explosive on the acceptor explosive is monitored by framing camera observation of the free surface behaviour of the acceptor, and in particular, by measurement of the axial blow-off velocity of the acceptor.

When chemical reaction occurs in the acceptor the free surface may either accelerate, decelerate, or stay at a constant velocity over the entire time, depending on the nature of the explosive acceptor and the degree of reaction. The free surface displacement of the acceptor, x_g , is measured frame by frame, and then the free surface velocity is obtained by measuring the slope, dx_g/dt , over a linear portion of the x_g-t curve, or at a point on the curve at a specified value of x_g if no linear portion exists. The value of x_g used was typically somewhere between 20 mm and 40 mm, but unfortunately does not appear to be specified in the reports, which makes detailed comparison with the simulated results difficult.

The MGT runs for H-6 were modelled using a Mie-Gruneisen equation of state for PMMA, as described by Bowman et al. [68], and the models for pentolite and H-6 described in section 6.2. The simulations were run in 2D cylindrical geometry using $\delta x = \delta y = 0.1$ cm and a fixed time step of 0.01 μs . Grid sizes were typically of the order of $n_x \times n_y = 240 \times 240$. The H-6 acceptor is 12.7 mm thick, the pentolite donor is 65 mm thick, and for H-6 the experimental results used PMMA gap lengths varying between 32.81 mm and 64.52 mm. Table 2 shows the input file `det.inp` for a MULTI run where the PMMA gap had a length of 35 mm.

Figure 7 shows the x_g-t curve for the simulated run, and Figure 8 shows the velocity-time plot obtained by numerically differentiating the curve, which shows that U_a changes continuously with time. The experimental value for U_a obtained by interpolation from the data reported by Liddiard and Forbes is 3.0 mm/ μs , but the location at which this velocity occurs is unknown. McIntosh [66] has modelled the MGT using a kinematic-isotropic elastic-plastic material model for PMMA and used the acceptor's maximum top surface velocity for comparison with the experimental results. If we adopt this approach we obtain $U_a = 3.1$ mm/ μs for a 35 mm gap, which agrees remarkably well with the experimental value, and is the same value as reported by McIntosh. For longer gap lengths the agreement is less encouraging, and reasons for the discrepancies are discussed in the paper by Jones [37].

Table 2: Input file *det.inp* for a typical MULTI run for the Modified GapTest.

```

NMAT
4
PBC
0.0
ALPHAX
1
ALPHAY
2
BCL, BCR, BCB, BCT
'R', 'T', 'R', 'T'
DELTAX
0.100
DELTAY
0.100
DELTAT, FIXED_TIME
0.0100, .true.
NCX
160
NCY
160
DEFEOS, DEFC0, DEFGAMMA, DEFRHO, DEFTMP
1, 0.03, 1.4, 1.0E-03, 3.0E2
DEFU0, DEFV0, DEFPRIORITY
0.0, 0.0, 4
INITTYPE, RADIUS
0, 0.0
XCENTRE, YCENTRE
0.0, 0.0
EOSTYPE(1), C0(1), GAMMA(1), RHO0(1), TMP0(1)
5, 0.0, 0.0, 1.70, 3.0E2
U0(1), V0(1), PRIORITY(1)
0.0, 0.0, 1
INITTYPE, RADIUS
0, 0.00
XCENTRE, YCENTRE
0.0, 0.0
IMIN(1), IMAX(1), JMIN(1), JMAX(1)
1, 65, 1, 25
ndumpx, ndumpy
0, 0
EOSTYPE(1), C0(1), GAMMA(1), RHO0(1), TMP0(1)
2, 0.2432, 1.0, 1.180, 3.0E2
U0(1), V0(1), PRIORITY(1)
0.0, 0.0, 2
INITTYPE, RADIUS
0, 0.0
XCENTRE, YCENTRE
0.0, 0.0
IMIN(1), IMAX(1), JMIN(1), JMAX(1)
66, 100, 1, 25
ndumpx, ndumpy
0, 0

```

```

EOSTYPE(1), C0(1), GAMMA(1), RHO0(1), TMP0(1)
3, 0.0, 0.0, 1.760, 3.0E2
U0(1), V0(1), PRIORITY(1)
0.0, 0.0, 3
INITTYPE, RADIUS
0, 0.0
XCENTRE, YCENTRE
0.0, 0.0
IMIN(1), IMAX(1), JMIN(1), JMAX(1)
101, 114, 1, 25
ndumpx, ndumpy
0, 0
MINSTEP
1
MAXSTEP
6000
IPRINT
100
PMIN
0.0
FULLDONOR
.TRUE.
DUMP, RESTART
.FALSE., .FALSE.
    
```

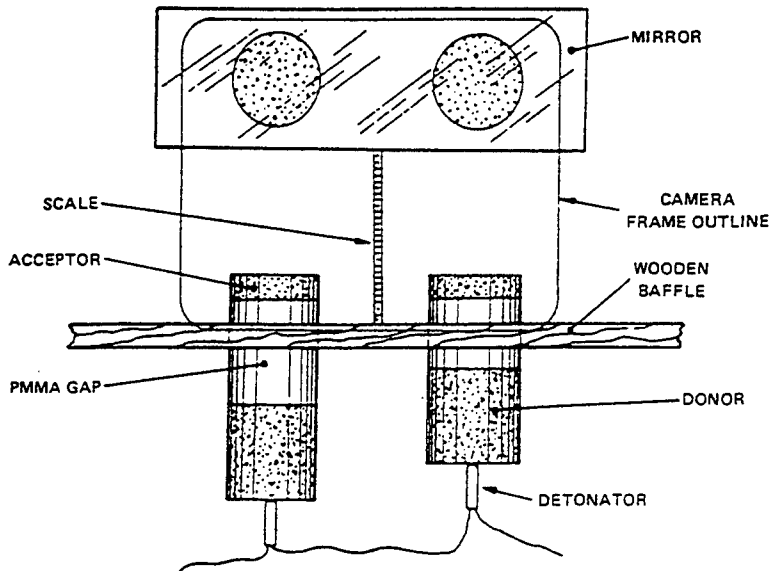


Figure 6: Schematic illustration of the Modified Gap Test Assembly.

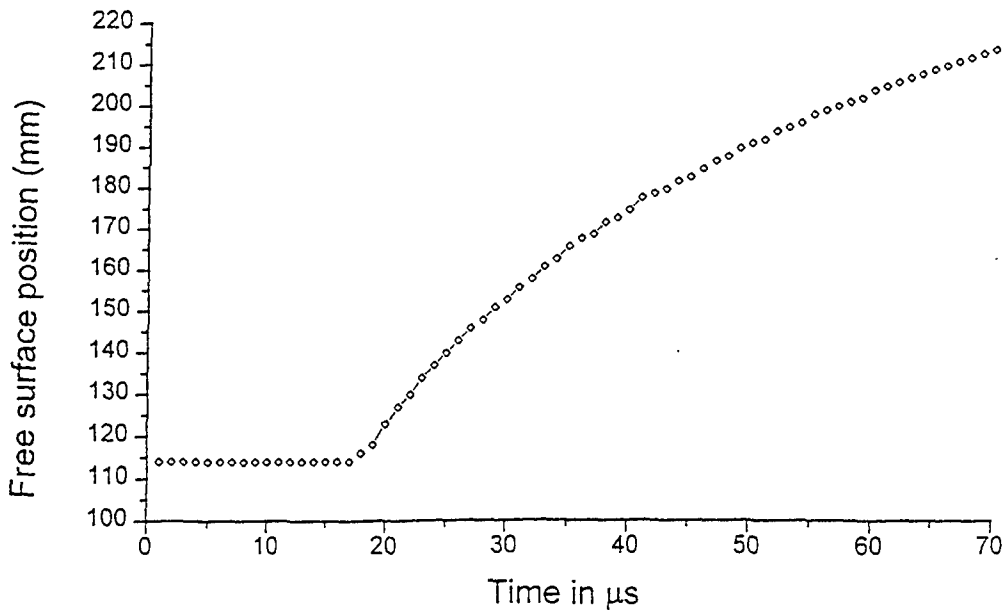


Figure 7. Plot of free surface position versus time for the MGT with a 35 mm PMMA gap length.

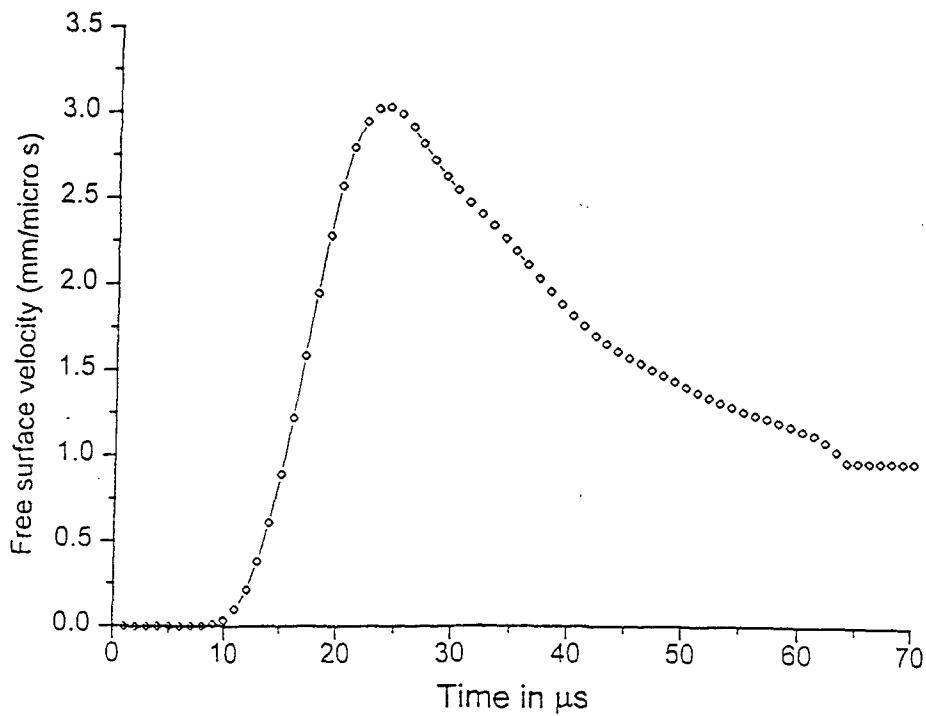


Figure 8. Plot of free surface velocity versus time for the MGT with a 35 mm PMMA gap length.

7. DISCUSSION AND CONCLUSION

During the time that MULTI has been under development a number of newer hydrocodes have become available. IFSAS (Integrated Fluid-Structure Analysis System) was developed by Combustion Dynamics Ltd. in Canada under contract to Defence Research Establishment Suffield [69]. IFSAS began as a pure Eulerian code to perform air blast calculations, but has grown considerably since then. Currently IFSAS contains a State module for basic gas dynamics calculations, a 3D CFD module for compressible flows, a Blast Raytracer module which uses image charge techniques to rapidly compute pressure loadings for internal explosions, and a finite element structural response module to compute elastic-plastic deformation of stiffened panels. Additional recent developments include implementation of a fully coupled Euler-Lagrange capability, and multiphase flow algorithms for both gaseous and condensed phase systems. Current developments include implementation of detonation and shock discontinuity trackers, and coupling with the LSTC DYNA3D finite element code.

CTH is an Eulerian code developed at Sandia National Laboratories to model three-dimensional, multimaterial, large deformation, strong shock wave physics [70]. CTH uses tabular or analytic equations of state to model solid, liquid, vapour, plasma, and mixed-phase materials. Material models include elastic-plastic behaviour, high explosives, fracture, and motion of fragments smaller than a computational cell. The 3D version of CTH uses a SLIC interface tracker, while the 2D version uses a high resolution interface tracker which assumes that the interface between two materials can be adequately approximated by a straight line. Explosives are described by a JWL equation of state and a programmed burn model.

CAST (Computational Applied Science and Technology) is a suit of computer programs which has been developed as a collaborative venture by Fluid Gravity Engineering Ltd. and the Defence Evaluation and Research Agency of the UK Ministry of Defence [71]. The basic modules provide a fully 2D/3D multi-material hydrocode capability including material strength and explosive modelling which is centred around the Euler codes EDEN and GRIM. These codes have the ability to model a wide range of structural dynamic problems, including impact studies, response to air blast, and response to underwater explosions. The CAST constitutive models take into account a variety of real material effects, including work hardening, thermal softening, and strain rate dependency. Other modules, such as a fully reactive flow capability, can also be added.

MESA is a 3D Eulerian code which treats hydrodynamic flow and the dynamic deformation of solid materials [72]. It was written at Los Alamos National Laboratory and was designed specifically for simulations of armour and anti-armour systems. It incorporates several of the standard strength models which take into account both the elastic and plastic regions of the stress-strain relationship of the materials. Explosives are described using a programmed burn model. MESA has been used to study the formation of non axisymmetric shaped charge jets, the penetration of reactive armour

by jets, and long rod penetrators. MESA contains highly accurate interface trackers which can resolve highly contorted deformations when only four computational cells are used to define plate thickness.

AUTODYN-2D and AUTODYN-3D were developed by Century Dynamics Ltd. and are interactive, integrated hydrocodes which provide a number of fully coupled numerical processors [73]. These include Lagrangian, Eulerian, Smooth Particle Hydrodynamics, and Arbitrary Lagrange Euler processors. The codes are particularly suited to the modelling of impact, penetration, blast and explosive events. The Euler codes use a version of the SLIC interface tracker to define material interfaces, and an artificial viscosity to spread shock fronts over several mesh intervals. Many material equations of state and material strength models are available in the codes. The strength models include Hydrodynamic, Elastic, Piecewise hardening, Brittle, and also the Johnson-Cook, Zerilli-Armstrong, Steinberg-Guinan and Johnson-Holmquist models, which include the effects of strain and strain hardening and thermal softening.

WSD staff are currently using IFSAS, LS-DYNA3D, and MULTI for a variety of simulation tasks in the areas of warhead simulation, blast/target interactions, and explosives simulation. IFSAS has a user friendly interface and is ideal to use when standard shock/material interaction problems need to be modelled. MULTI, on the other hand, was designed to provide an in-house code which could be quickly adapted to model more novel explosive/shock problems. Recent examples within WSD have included the design and implementation of an energetic model for the explosive PBXN-111 (formerly PBXW-115) [56], and fully three-dimensional air blast simulations [28]. MULTI is written in FORTRAN and runs from a standard input data file, as the examples in the previous section have shown, but users are expected to be familiar with CFD techniques and to be capable of modifying the coding when non-standard problems arise. The ability to modify the source code in this way is one of the advantages of MULTI which is not shared by the more commercial codes listed above, although some of them, for example AUTODYN and CAST, do allow users to write their own subroutines to specify particular material models. A further advantage of an in-house code such as MULTI is the ability to tailor the code to suit the architecture of whichever computer system is available at the time. For example, a simplified version of MULTI has already been configured to run in parallel mode on the AMRL POWER CHALLENGE XV [74]. Further development of MULTI will depend on the interests and expertise of WSD staff, and the future direction of WSD tasks.

8. ACKNOWLEDGMENTS

The authors wish to thank A. Milne and W. Carnegie of Fluid Gravity Engineering Ltd. for providing considerable assistance with parts of the coding, and M.C. Chick of WSD, AMRL, for enthusiastically supporting this work.

9. REFERENCES

1. Mader, C.L. and Gage, W.R. (1967) "FORTRAN SIN-A One-Dimensional Hydrodynamic Code for Problems Which Include Chemical Reaction, Elastic-Plastic Flow, Spalling, and Phase Transitions", Los Alamos National Laboratory report LA-3720.
2. Johnson, J.N., Mader, C.L. and Shaw, M.S. (1981) "2DL: A Lagrangian Two-Dimensional Finite Difference Code for Reactive Media", Los Alamos National Laboratory report LA-8922-M.
3. Kershner, J.D. and Mader, C.L. (1972) "2DE: A Two-Dimensional Continuous Eulerian Hydrodynamic Code for Computing Multi component Reactive Hydrodynamic Problems", Los Alamos National Laboratory report LA-4846.
4. Mader, C.L. and Kershner, J.D. (1980) "Three-Dimensional Eulerian Calculations of Triple Initiated PBX 9404", Los Alamos National Laboratory report LA-8206.
5. Mader, C.L. (1979) Numerical Modelling of Detonations, University of California Press, Berkely
6. Hageman, L.J. (1976) "HELP-A Multimaterial Eulerian Program in Two Space Dimensions and Time", Systems, Science and Software, AFATL-TR-76-45.
7. Durrett, R.E. and Matuska, D.A. (1978) "The HULL Code, Finite Difference Solution to the Equations of Continuum Mechanics", Air Force Armament Laboratory, AFATL-TR-78-125.
8. Hallquist, J.O. (1984) "User's Manual for Dyna2D - an Explicit, Two Dimensional Finite Element Code with Interactive Rezoning", Lawrence Livermore National Laboratory report, UCID-18756, Rev. 2.
9. Macintyre, I. and Smith, D. (1986). "Collapse of the MRL 38 mm Shaped Charge - A Data Base for Computer Modelling", MRL-R-1025
10. Masinskas, J.J. and Van Leeuwen, E H. (1987) "Theoretical Investigation of the wave shaping process in a section of ladder Fracture Tape", MRL Report, MRL-R-1081.
11. Janzon, B. (1993) "Numerical Calculation of Collapse and Jet data for the MRL 38 mm Shaped Charge using PC-DYNA2D", MRL Technical Report MRL-TR-93-29.
12. Janzon, B. (1993) "Modelling Explosively Formed Penetrators and Shaped Charges on Personal Computers using PC-DYNA2D", MRL Technical Report MRL-TR-93-28.
13. Lam, C. and McQueen, D. (1996) "Numerical Simulation of the Formation and Penetration of Explosively Formed Projectiles", Computational Techniques and Applications: CTAC95, pp. 433-440, Eds. R.L. May and A.K. Easton, World Scientific Publishing Co.

14. Thornton, D.M, Lam, C. and Chick, M. (1996) "Underwater Warhead Damage Mechanisms to Ship Hulls", 16th International Symposium on Ballistics, San Francisco, Ca.
15. Boris, J.P. and Book, D.L. (1976) "Solution of Continuity Equations by the Method of Flux-Corrected Transport" Chap. 11, Vol. 16, Methods of Computational Physics, Academic Press, New York.
16. Oran, E.S. and Boris, J.P. (1987) *Numerical Simulation of Reactive Flow*, Elsevier, New York
17. Jones, D.A., Guirguis, R. and Oran E.S. (1989) "Numerical Simulation of Detonation Transfer Between Gaseous Explosive Layers", MRL Research Report, MRL-RR-1-89.
18. Jones, D.A, Sichel, M., Oran, E.S. and Guirguis, R. (1990) "Detonation Transmission in Layered Explosives", Proceedings of The Twenty Third Symposium (International) on Combustion, The Combustion Institute, PA.
19. Jones, D.A., Sichel, M., Guirguis, R. and Oran, E.S. (1991) "Numerical Simulation of Layered Detonations", Progress in Astronautics and Aeronautics, **133**, 202-220.
20. Tyndall, M.B. (1989) "Numerical Modelling of Shocks in gases and metals", MRL Research Report, MRL-RR-8-89.
21. Tyndall, M.B., (1993) "Numerical modelling of shocks in solids with elastic-plastic conditions", *Shock Waves*, **3**: 55-66.
22. Jones, D.A., Oran, E.S. and Guirguis, R. (1990). "A One-Dimensional Flux-Corrected Transport Code for Detonation Calculation". MRL Research Report, MRL-RR-2-90.
23. Oran, E.S., Jones, D.A. and Sichel, M. (1992) "Numerical Simulation of Detonation Transmission". Proc. Roy. Soc. A, **436**, 267-297
24. Oran. E.S., Boris, J.P., Jones, D.A. and Sichel, M. (1993) "Ignition in a Complex Mach Structure", Progress in Astronautics and Aeronautics, **153**, 241-252
25. Jones, D.A., Oran, E.S., and Sichel, M. "Reignition of Detonation by Reflected Shocks", *Shock Waves*, **5**, 47-57, 1995.
26. Jones, D.A., Kemister, G., Oran, E.S, Sichel, M. (1996) "The Influence of Cellular Structure on Detonation Transmission", *Shock Waves*, **6**, 119 - 130.
27. Jones, D.A. (1992) "Blast Overpressure Calculations for Wall Breaching Charges" Proceedings of the TTCP TLG-3 Blast/Thermal Symposium, Vol. 1, 10-1 to 10-9
28. Kemister, K. (1995) "Computational Fluid Dynamics Modelling of the Australian Challenge", DSTO Technical Report DSTO-TR-0224.
29. Winter, P.L., Thornton, D.M., Learmonth, L.A., Jones, D.A., Kemister, G. and Ritzel, D.V. (1995) "Measurement and Simulation of Air Blast Hazards Associated with Door Breaching Operations", *Proceedings of the Military Aspects of Blast Symposium*, Las Cruces, NM.

30. Jones, D.A., Kemister, G. and Ritzel, D.V. (1995) "Blast Overpressure Calculations for Door Breaching Charges", *DSTO Technical Report*, DSTO-TR-0245, 32 pp.
31. Kemister, G. and Jones, D.A. (1996) "Numerical Simulation of Blast Overpressures around Buildings", *Computational Techniques and Applications: CTAC-95*, Eds. R. May and A. Easton, World Scientific Publishing, pp 425 - 432.
32. Milne, A.M. and Carnegie, W.D. (1993) "Implementation of a Simple Line Interface Calculation (SLIC) Scheme for use with LCPFCT" Fluid Gravity Engineering Report CR 102/93
33. Carnegie, W.D. (1994) *An Improved SLIC Scheme for LCPFCT, Incorporating Multi-Material Thermodynamics*, Fluid Gravity Engineering Ltd., Report CR 102/94.
34. Doyle, A., Jones, D.A. and Kemister, G (1996) "Colour Graphics for Hydrocode Simulations", *DSTO General Document*, DSTO-GD-0059, 51 pp.
35. Borg, R.A.J. and Jones, D.A. (1996) "A Multi-material Eulerian Hydrocode for Explosive/ Material Interactions", *Computational Techniques and Applications: CTAC-95*, Eds. R. May and A. Easton, World Scientific Publishing, pp 145 - 152.
36. Borg, R.A.J. and Jones, D.A. (1996) "Numerical Simulation of Bullet Impact Experiments using the Forest Fire Reaction Rate Model", *DSTO Technical Report*, DSTO-TR-0325, 25 pp.
37. Jones, D.A. (1998) "Numerical Simulation of H6 Sensitivity Tests", Paper presented at the TTCP KTA 1-28 meeting, Naval Air Warfare Center, China Lake, May 1998.
38. Meyers, M.A. (1994) *Dynamic Behaviour of Materials*, John Wiley and Sons, Inc.
39. Thompson, P.A. (1972) "Compressible Fluid Dynamics", McGraw-Hill, Inc.
40. Tran, D., Link, R., Penrose, J. and Thibault, P.A. (1994) "CFD Modeling of Fluid-Structure and Liquid-Gas Interactions", *Proceedings of the 2nd Canadian CFD Conference*, UTIAS, Toronto, pp. 171 -178.
41. Borg, R.A.J., Kemister, G. and Jones, D.A. (1995) "Chemical Equilibrium Calculations for Detonation Products", *DSTO Technical Report*, DSTO-TR-0226, 40 pp.
42. Lee, E.L., Hornig, H.C. and Kury, J.W. (1968) *Adiabatic Expansion of High Explosive Detonation Products* *Lawrence Livermore Laboratory Report* UCRL-50422.
43. Dobratz, B.M. and Crawford, P.C. (1985) *LLNL Explosives Handbook*, *Lawrence Livermore National Laboratory report*, UCRL-52997.
44. Karpp, R.R. (1993) "Warhead Simulation Techniques: Hydrocodes", in *Tactical Missile Warheads*, J. Carleone, ed. *Progress in Astronautics and Aeronautics*, 155, pp. 233 - 314.
45. Jones, D.A. (1989) "A Critical Assessment of Models Available for the Shock Initiation of Heterogeneous Explosives", *MRL Technical Report*, MRL-TR-89-17.

46. Mader, C.L. and Forest, C.A. (1976) Two-Dimensional Homogeneous and Heterogeneous Detonation Wave Propagation, Los Alamos Scientific Laboratory Report LA-6259.
47. Ramsay, J.B. and Popolato, A. (1965) Analysis of Shock Wave and Initiation Data for Solid Explosives, *Proceedings of the Fourth Symposium (International) on Detonation*, Office of Naval Research, ACR-126, pp. 233-238.
48. Starckenberg, J (1993) "An Assessment of the Performance of the Original and Modified Versions of the Forest Fire Explosive Initiation Model", *Proceedings of the Tenth International Detonation Symposium*, Boston. Office of Naval Research, ONR 33395-12, pp. 992 - 1002.
49. Lundstrom, E.A. (1988) "Evaluation of Forest Fire Burn Model of Reaction Kinetics of Heterogeneous Explosives", Naval Weapons Centre Technical Publication 6898.
50. Liang, D., Flis, W.J., and Chou, P.C. (1993) "The Calculation of the Constants for the Forest Fire Model", *Proceedings of the Tenth International Detonation Symposium*, Boston, Office of Naval Research, ONR 33395-12, pp. 1003-1009.
51. Lee, E.L. and Tarver, C.M. (1980) "Phenomenological Model of Shock Initiation in Heterogeneous Explosives, *Physics of Fluids*, **23**, 2362-2372.
52. Tarver, C.M., Hallquist, J.O, and Erickson, L.M. (1985) Modelling short pulse duration shock initiation of solid explosives, *Proceedings of the Eighth Symposium (International) on Detonation*, Albuquerque, New Mexico, pp. 951 - 961.
53. Murphy, M.J., Lee, E.L., Weston, A.M. and Williams, E.A. (1993) Modelling Shock Initiation in Composition B, *Proceedings of the Tenth International Detonation Symposium*, Boston, Office of Naval Research, ONR 33395-12, 963-970.
54. Miller, P.J. (1996) A Simplified Method for Determining Reactive Rate Parameters for Reaction Ignition and Growth in Explosives, *Research Department, Naval Air Warfare Center, Weapons Division, China Lake, CA 93555-6001*, preprint.
55. P.J. Miller, P.J. and G.T. Sutherland, G.T. (1996) Reaction Rate Modelling of PBXN-110, *Shock Compression of Condensed Matter - 1995*, AIP Conference Proceedings 370, Part 1, S.C. Schmidt and W.C. Tao, eds., 413-416.
56. Kennedy, D.L and Jones, D.A. (1993) "Modelling Shock Initiation and Detonation in the Non-Ideal Explosive PBXW-115", *Proceedings of the Tenth International Detonation Symposium*, Boston, Office of Naval Research, ONR 33395-12, pp. 665-674.
57. Kirby, I.J. and Leiper, G.A. (1985) "A small divergent detonation theory for intermolecular explosives", *Proceedings of the Eighth Symposium (International) on Detonation*, Albuquerque, pp. 176-185.
58. Afanesenkov, A.N., Bolomolar, V.M., and Voskoboinikov, I.M. (1969). Generalised shock Hugoniot of condensed substance. *Zhur. Proc. Mekh. Tekh. Fig. 10*, pp.137 - 147.
59. Boris, J.P, Landsberg, A.M., Oran, E.S. and Gardner, J.H. (1993) "LCPFCT - A Flux-Corrected Transport Algorithm for Solving Generalized Continuity Equations", *Naval Research Laboratory report NRL/MR/6410—93-7192*.

60. Noh, W.F. and Woodward, P. (1976) "The SLIC (Simple Line Interface Calculation) Method" UCRL-52111.
61. Youngs, D.L. (1982) "Time Dependent Multi-Material Flow with Large Fluid Distortion", Numerical Methods for Fluid Dynamics, KW Morton and MJ Bains (eds).
62. Guirguis, R. and Oran, E.S. (1983) "Reactive Shock Phenomena in Condensed Materials: Formulation of the Problem and Method of Solution". Naval Research Laboratory Memorandum Report 5228.
63. Starkenberg, J., Huang, Y., and Arbuckle, A. (1983) "Numerical Modelling of Projectile Impact Shock Initiation of Bare and Covered Composition-B", Journal of Energetic Materials, 2, Number 1-2, pp 1-42.
64. Slade, D.C. and Dewey, J. (1957) *High-Order Initiation of two Military Explosives by Projectile Impact*, Ballistics Research Laboratory Report No. 1021, July 1957.
65. Liddiard, T.P. and Forbes, J.W. (1987) "A Summary Report of the Modified Gap Test and the Underwater Sensitivity Test", *Naval Surface Warfare Center report*, NSWC TR 86-350.
66. McIntosh, G. (1998) Modelling of the Explosive H-6, Defence Research Establishment Valcartier, Quebec, Report DREV-TM-9802, pp.15, March 1998.
67. Hudson, L.C. (1992) Computational Studies of Sympathetic Detonation between Two Axially Adjacent, Cased Charges of H-6, in *Shock Compression of Condensed Matter - 1991*, Schmidt, S.C. et al. Eds., Elsevier Science Publishers, Amsterdam.
68. Bowman, A.L., Kershner, J.D. and Mader, C.L. (1980) "A Numerical Model of the Gap Test", *Los Alamos Scientific Laboratory report*, LA-8408.
69. Thibault, P and Sulmistras, A. (1992) "Fluid Dynamics/Blast Prediction & Structural Response Workstation", Proceedings of the TTCP TLG-3 Blast/Thermal Symposium, Melbourne, May 26-28, 1992.
70. McGlaun, J.M., Thompson, S.L. and Elrick, M.G. (1990) "CTH: A Three-dimensional Shock Wave Physics Code", International Journal of Impact Engineering, 10, 351-360.
71. Cullis, I.C. (1997) Personal communication, September 1997.
72. Cort, E. (1989) "Modeling Armor Penetration", Los Alamos Science, Number 17, 64-67.
73. O'Grady, H.J.P., Hayhurst, C.J. and Fairlie, G.E. (1996) "The Numerical Simulation of Warheads, Impact and Blast Phenomena using AUTODYN-2D and AUTODYN-3D", Proceedings of the South African Ballistics Symposium, Stellenbosch, South Africa, November 1996.
74. Weapons Systems Division Task Progress Report for Period January 1997 to June 1997 for the Task "Hydrocode Development for Target Encounter Modelling", DST 96/142.

DISTRIBUTION LIST

Numerical Simulation of Detonation In Condensed Phase Explosives

D.A. Jones, G. Kemister and R.A.J. Borg
AUSTRALIA

DEFENCE ORGANISATION

S&T Program

Chief Defence Scientist
FAS Science Policy
AS Science Corporate Management
Director General Science Policy Development
Counsellor Defence Science, London (Doc Data Sheet)
Counsellor Defence Science, Washington (Doc Data Sheet)
Scientific Adviser to MRDC Thailand (Doc Data Sheet)
Director General Scientific Advisers and Trials/Scientific Adviser Policy and
Command (shared copy)
Navy Scientific Adviser (Doc Data Sheet and distribution list only)
Scientific Adviser - Army (Doc Data Sheet and distribution list only)
Air Force Scientific Adviser
Director Trials

} shared copy

Aeronautical and Maritime Research Laboratory

Director

Chief of Weapons Systems Division

Dr D.A. Jones, MPD

Dr G. Kemister, AOD

Dr. R.A.J. Borg, KODAK Australia

Mr. D.V. Ritzel, WSD

Dr. A. Wildegger-Gaissmaier, WSD

Dr. K. Matthews, WSD

Dr. W. Wilson, WSD

Dr. H. Dorsett, WSD

Dr. S.Y. Ho, WSD

DSTO Library

Library Fishermens Bend

Library Maribyrnong

Library Salisbury (2 copies)

Australian Archives

Library, MOD, Pyrmont (Doc Data sheet only)

Capability Development Division

Director General Maritime Development (Doc Data Sheet only)

Director General Land Development (Doc Data Sheet only)

Director General C3I Development (Doc Data Sheet only)

Army

ABCA Office, G-1-34, Russell Offices, Canberra (4 copies)
SO (Science), DJFHQ(L), MILPO Enoggera, Queensland 4051 (Doc Data Sheet only)
NAPOC QWG Engineer NBCD c/- DENGERS-A, HQ Engineer Centre Liverpool Military Area, NSW 2174 (Doc Data Sheet only)

Intelligence Program

DGSTA Defence Intelligence Organisation

Corporate Support Program (libraries)

OIC TRS, Defence Regional Library, Canberra
Officer in Charge, Document Exchange Centre (DEC) (Doc Data Sheet and distribution list only)
*US Defence Technical Information Center, 2 copies
*UK Defence Research Information Centre, 2 copies
*Canada Defence Scientific Information Service, 1 copy
*NZ Defence Information Centre, 1 copy
National Library of Australia, 1 copy

UNIVERSITIES AND COLLEGES

Australian Defence Force Academy
Library
Head of Aerospace and Mechanical Engineering
Deakin University, Serials Section (M list), Deakin University Library, Geelong, 3217
Senior Librarian, Hargrave Library, Monash University
Librarian, Flinders University

OTHER ORGANISATIONS

NASA (Canberra)
AGPS
Dr. David Kennedy, ORICA, NSW

OUTSIDE AUSTRALIA

Dr. Elaine Oran, NRL, Washington, DC
Dr. Alec Milne, Fluid Gravity Engineering Ltd., UK
Dr. Paul Thibault, Combustion Dynamics Ltd., Canada
Dr. David Frost, McGill University, Canada
Dr. Martin Sichel, University of Michigan, USA

ABSTRACTING AND INFORMATION ORGANISATIONS

INSPEC: Acquisitions Section Institution of Electrical Engineers
Library, Chemical Abstracts Reference Service
Engineering Societies Library, US
Materials Information, Cambridge Scientific Abstracts, US
Documents Librarian, The Center for Research Libraries, US

INFORMATION EXCHANGE AGREEMENT PARTNERS

Acquisitions Unit, Science Reference and Information Service, UK
Library - Exchange Desk, National Institute of Standards and Technology, US

SPARES (10 copies)

Total number of copies: 65

DEFENCE SCIENCE AND TECHNOLOGY ORGANISATION DOCUMENT CONTROL DATA				1. PRIVACY MARKING/CAVEAT (OF DOCUMENT)	
2. TITLE NUMERICAL SIMULATION OF DETONATION IN CONDENSED PHASE EXPLOSIVES			3. SECURITY CLASSIFICATION (FOR UNCLASSIFIED REPORTS THAT ARE LIMITED RELEASE USE (L) NEXT TO DOCUMENT CLASSIFICATION) Document (U) Title (U) Abstract (U)		
4. AUTHOR(S) D.A. Jones, G. Kemister and R.A.J. Borg			5. CORPORATE AUTHOR Aeronautical and Maritime Research Laboratory PO Box 4331 Melbourne Vic 3001 Australia		
6a. DSTO NUMBER DSTO-TR-0705		6b. AR NUMBER AR-010-605		6c. TYPE OF REPORT Technical Report	
7. DOCUMENT DATE August 1998					
8. FILE NUMBER 510/207/0915		9. TASK NUMBER DST 96/142		10. TASK SPONSOR DST	
			11. NO. OF PAGES 40		12. NO. OF REFERENCES 74
13. DOWNGRADING/DELIMITING INSTRUCTIONS			14. RELEASE AUTHORITY Chief, Weapons Systems Division		
15. SECONDARY RELEASE STATEMENT OF THIS DOCUMENT <i>Approved for public release</i> OVERSEAS ENQUIRIES OUTSIDE STATED LIMITATIONS SHOULD BE REFERRED THROUGH DOCUMENT EXCHANGE CENTRE, DIS NETWORK OFFICE, DEPT OF DEFENCE, CAMPBELL PARK OFFICES, CANBERRA ACT 2600					
16. DELIBERATE ANNOUNCEMENT No Limitations					
17. CASUAL ANNOUNCEMENT			Yes		
18. DEFTEST DESCRIPTORS hydrocodes, detonation, explosives, numerical simulation, reactive hydrocodes, reactive simulations, multimaterial hydrocodes, bullet impact, underwater explosives, gap test					
19. ABSTRACT This report describes the development of a two-dimensional multi-material Eulerian hydrocode to model the effects of detonating condensed phase explosives on surrounding materials. The code solves the Euler equations for the conservation of mass, momentum, and energy for an inviscid, compressible fluid. Operator splitting is used to reduce the two-dimensional calculation into coupled one-dimensional equations, which are then solved using the Flux-Corrected Transport (FCT) algorithm of Boris and Book. Non-reacting materials are described using either a perfect gas, Mie-Gruneisen, or Tait equation of state, while the energetic materials are described using either a BKW equation of state and Forest Fire reaction rate model, or the JWL equation of state and the Ignition and Growth reaction rate model. A modified Young's algorithm is used to maintain a sharp interface between different materials on the computational mesh. A brief description of the major components of the coding is provided, and then several applications of the code are described, including the simulation of bullet impact experiments, the underwater sympathetic detonation test, and the modified gap test.					